Theoretical and experimental studies of the ZnSe/CuInSe2 heterojunction band offset

Art J. Nelson, C. R. Schwerdtfeger, Su-Huai Wei, Alex Zunger, D. Rioux, R. Patel, and Hartmut Höchst

Articles you may be interested in

Tuning of ZnSe–GaAs band discontinuities in heterojunction diodes
Appl. Phys. Lett. **69**, 3233 (1996); 10.1063/1.118020

Polarization fields and band offsets in GaInP/GaAs and ordered/disordered GaInP superlattices
Appl. Phys. Lett. **68**, 2852 (1996); 10.1063/1.116346

Band alignment at the CdS/Cu2In4Se7 heterojunction interface
Appl. Phys. Lett. **67**, 2969 (1995); 10.1063/1.114828

Photoemission investigation of the ZnSe/CdTe heterojunction band discontinuity
J. Appl. Phys. **78**, 2537 (1995); 10.1063/1.360109

Band offsets at the CdS/CuInSe2 heterojunction
Appl. Phys. Lett. **63**, 2549 (1993); 10.1063/1.110429

Theoretical and experimental studies of the ZnSe/CuInSe$_2$ heterojunction band offset

Art J. Nelson, C. R. Schwerdtfeger, Su-Huai Wei, and Alex Zunger
National Renewable Energy Laboratory, Golden, Colorado 80401

D. Rioux, R. Patel, and Hartmut Höchst
Synchrotron Radiation Center, University of Wisconsin-Madison, Stoughton, Wisconsin 53589

We report first-principles band structure calculations that show that ZnSe/CuInSe$_2$ has a significant valence band offset (VBO, ΔE_v): 0.70±0.05 eV for the relaxed interface and 0.60±0.05 eV for the coherent interface. These large values demonstrate the failure of the common anion rule. This is traced to a stronger Cu,d-Se,p level repulsion in CuInSe$_2$ than the Zn,d-Se,p repulsion in ZnSe. The VBO was then studied by synchrotron radiation soft x-ray photoemission spectroscopy. ZnSe overlayers were sequentially grown in steps on n-type CuInSe$_2$(112) single crystals at 200 °C. *In situ* photoemission measurements were acquired after each growth in order to observe changes in the valence band electronic structure as well as changes in the In $4d$ and Zn $3d$ core lines. Results of these measurements reveal that the VBO is ΔE_v=0.70±0.15 eV, in good agreement with the first-principles prediction.

The ternary $A^I B^{III} X_2^{VI}$ chalcopyrite semiconductor, CuInSe$_2$ (E_g=1.1 eV), has received considerable attention as an absorber in heterojunction solar cells.[1] Technical advances in polycrystalline thin-film technology have demonstrated photovoltaic devices with efficiencies exceeding 14%.[1] The theoretical electronic structure of CuInSe$_2$ has been calculated[2] and experimental data have confirmed the electronic band structure.[3] In addition, the wide band gap II-VI semiconductor ZnSe (E_g=2.67 eV) has promising applications as a window layer for photovoltaic heterojunctions.[4]

The ZnSe/CuInSe$_2$ heterojunction provides an interesting test case for our understanding of the physics of band offsets: like AlAs/GaAs and CdTe/HgTe, it too is nearly (2%) lattice matched, and has a common anion. By the common anion rule[5] it is thus expected to have a vanishing valence band offset. We now know[6] that this rule is violated in the above two cases involving *binary* heterojunction partners. ZnSe/CuInSe$_2$ is the first nearly lattice matched, common-anion system consisting of a *ternary* heterojunction partner to be tested in this respect. This system is interesting because it involves a near-transition metal atom (copper): the failure of the common-anion rule in Zn, Cd, and Hg containing II-VI heterojunctions was attributed[6] to the different repulsion between the cation d orbitals and the common anion p orbitals on either side of the interface. Since the d band in Cu has a much lower binding energy than the d band in Zn, Cd, and Hg-based II-VIs,[2] there is a correspondingly large difference in the p-d level repulsions in CuInSe$_2$ and II-VI materials. Hence, Cu-containing heterojunctions with II-VI semiconductors should exhibit a greater departure from the common-anion rule than pure II-VI heterojunctions. Progress in attaining a comprehensive understanding of heterojunction band discontinuities is necessary in order to ultimately control these interfacial properties. This letter discusses theoretical predictions of the ZnSe/CuInSe$_2$ heterojunction band discontinuity and the results of a soft x-ray photoemission investigation of heterojunction formation.

We have first calculated the valence band offset (VBO) in ZnSe/CuInSe$_2$, then measured it. Previous theories of band offsets[7-10] did not address the case where one heterojunction partner is a ternary compound.

The band offset between two materials ABX_2 and DX can be expressed as (see Fig. 1):

$$\Delta E_{vbm} = \Delta E_{vbm,c}^{ABX_2} - \Delta E_{vbm,c}^{DX} - \Delta E_c, \qquad (1)$$

where $\Delta E_{vbm,c}^{ABX_2} = E_{vbm}^{ABX_2} - E_c^{ABX_2}$ and $\Delta E_{vbm,c}^{DX} = E_{vbm}^{DX} - E_c^{DX}$ are the core-level (c) to the valence band maximum (vbm) energy separations for materials ABX_2 and DX, respectively, and $\Delta E_c = E_c^{DX} - E_c^{ABX_2}$ is the difference in core-level binding energy between ABX_2 and DX on the two sides of the interface. We calculate the band offset for the ZnSe/CuInSe$_2$ heterojunction in an analogous way to previous calculations on binary systems.[6] We have performed first-principles total energy and band structure calculations for the constituents CuInSe$_2$ and ZnSe, obtaining the three
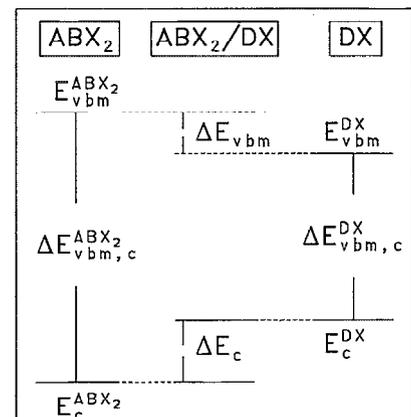
FIG. 1. Schematic energy-level diagram used to deduce the valence band offset between ABX_2 and DX.
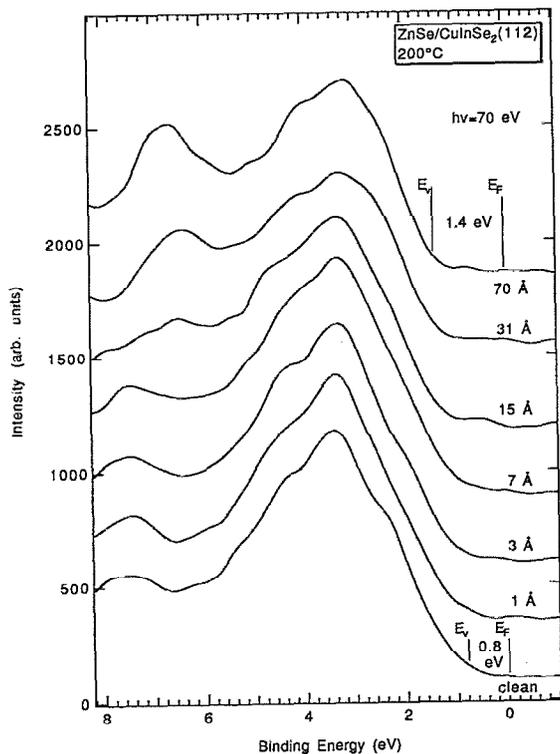
FIG. 2. Normal emission valence band spectra of the ZnSe/CuInSe$_2$ interface as a function of the effective ZnSe coverage for the n-type crystals. Zero of energy is at E_F.

FIG. 3. Characteristic core level emission for CuInSe$_2$ as a function of the effective ZnSe coverage (a) In 4d and (b) Zn 3d. Zero of energy is at E_F.

terms of Eq. (1). The two core-to-vbm energy differences $\Delta E_{vbm,c}$ were obtained as eigenvalue differences in separate calculations on CuInSe$_2$ and ZnSe. The core-level difference ΔE_c between the two materials was obtained from band calculations on the (CuInSe$_2$)$_p$/(ZnSe)$_{2p}$ superlattices with (001) orientation. In this superlattice calculation the number of layers p was increased until the core energy levels of the innermost layer on each side of the interface were bulklike. We found that for $p=2$ the uncertainty associated with using different core levels (e.g., the anion 1s or the cation 1s) was less than 0.05 eV. The band calculations were performed using the density functional formalism[11] as implemented by the general potential, relativistic, all electron linear augmented plane wave (LAPW) method.[12] We use the Ceperly–Alder exchange correlation potential as parameterized by Perdew and Zunger.[13] The Brillouin zone integrations are performed using ten special **k** points for the zinc-blende zone and their equivalent **k** points for the superlattice structures.[14] The equilibrium atomic structures at the interface were determined through total energy minimization and quantum mechanical force calculations. The calculated equilibrium lattice constants for CuInSe$_2$ and ZnSe are 5.736 Å (observed: 5.784 Å)[15] and 5.618 Å (observed; 5.667 Å),[16] respectively. The calculated tetragonal distortion $c/a=1.008$ and internal relaxation $u=0.214$ in CuInSe$_2$ can be compared with the observed[15] values of 1.004 and 0.224, respectively.

The calculated VBO depends on the interfacial geometry. We considered two limiting cases: (i) the interface is relaxed, so each heterojunction partner attains its own equilibrium atomic geometry. This gives $\Delta E_{vbm}=0.70 \pm 0.05$ eV with the vbm of CuInSe$_2$ above that of ZnSe. In the absence of strain, $\Delta E_{cbm}=E_g^{(1)} - E_g^{(2)} - \Delta E_{vbm}=0.90 \pm 0.05$ eV, where $E_g^{(1)}$ and $E_g^{(2)}$ are the bulk band gaps of DX and ABX_2. (ii) ZnSe is assumed to be coherently strained onto the (112) face of the CuInSe$_2$ substrate. In this case we find that the vbm of ZnSe is split by a crystal field effect; the upper split component moves to lower binding energy by 0.1 eV, hence $\Delta E_{vbm}=0.60 \pm 0.05$ eV. The tensile strain in ZnSe further lowers its cbm by 0.1 eV, so $\Delta E_{cbm}=0.80 \pm 0.05$ eV. Note that in the presence of strain $\Delta E_{cbm} \neq E_g^{(1)} - E_g^{(2)} - \Delta E_{vbm}$.

These large band offsets between CuInSe$_2$ and ZnSe are clearly in contradiction with the old common-anion rule,[5] which states that for a common anion system the valence band offset is small. In fact, this appears to be the largest departure from this rule yet. The breakdown of the common-anion rule for this system is due to the strong cation d orbital admixture in the vbm: in the zinc-blende structure, the anion p and the cation d orbitals have the same $t_2(\Gamma_{15v})$ symmetry at the zone center, hence they can couple and mix with each other. The same is true for CuInSe$_2$. This coupling repels the two levels, pushing the vbm to lower binding energies by an amount inversely proportional to the (metal-d) to (nonmetal-p) energy difference. In CuInSe$_2$, the Cu 3d orbitals have a much smaller binding energy than the Zn 3d orbitals in ZnSe, so the (Cu,3d)-(Se,4p) coupling in CuInSe$_2$ is much stronger than the (Zn,3d)-(Se,4p) coupling in ZnSe. This interaction pushes the vbm of CuInSe$_2$ up in energy relative to the vbm of ZnSe. In the absence of this effect, the common

anion rule should apply. We have tested this mechanism by artificially turning off the *p-d* coupling in the LAPW calculation. We find that in this case $\Delta E_{vbm} \approx 0$, as expected from the common-anion rule. This establishes *p-d* coupling as the source of failure of the common-anion rule in ZnSe/CuInSe$_2$. A similar conclusion was previously reached for CdTe/HgTe,[6] except that the differential *p-d* coupling is considerably stronger in the ternary case.

This prediction, obtained prior to experimental testing, was tested by the photoemission measurements described next. The CuInSe$_2$ crystals were sliced from an ingot which was prepared by high-pressure liquid-encapsulated direction solidification (LEDS).[17] The samples were polished with bromine-methanol and exhibited 0.5–1.5 cm grain sizes. Laue backscattering and x-ray photoemission from a single grain confirmed the (112) surface orientation and stoichiometry. The crystal surface was sputter cleaned with 500 eV Ar ions, 30° incidence followed by annealing for ≈ 2 min at 500 °C to remove sputter-induced damage.

The ZnSe overlayers were deposited in steps on *n*-type CuInSe$_2$ at 200 °C using a liquid nitrogen shrouded boron nitride effusion cell (750 °C). Photoemission spectra were obtained after each growth in order to observe the development of the electronic structure at the heterojunction interface. These experiments were performed using the Amoco 6m torodial grating monochromator (TGM) at the University of Wisconsin Synchrotron Radiation Center. The photoemitted electrons were analyzed using a hemispherical sector analyzer and were measured at normal emission with $h\nu = 70$ eV and an energy resolution of $\Delta E \approx 0.1$ eV.

Figure 2 shows the normal emission valence band spectra of the ZnSe/CuInSe$_2$ interface as a function of the effective ZnSe coverage. The observed upper valence band appears as a two peak structure corresponding to the two branches of the Cu *d* bands. The transition of the valence band maximum shown here is a direct indication of the evolution of the electronic structure leading to the ZnSe/CuInSe$_2$ heterojunction formation. The positions of the *vbm* for CuInSe$_2$ and ZnSe are determined from the linear extrapolation of the leading edge of the clean spectrum and the 70 Å ZnSe spectrum, respectively. For the clean CuInSe$_2$, we observe $E_F - E_{vbm} = 0.8$ eV while for the ZnSe covered surface $E_F - E_{vbm} = 1.4$ eV. Since the bulk crystal is *n*-type, the cleaned CuInSe$_2$ bands are very nearly flat near the surface with minimal (<0.2 eV) band bending. No significant shift is observed in the dominant Cu *d* band features which indicates that the flat band condition remains in the CuInSe$_2$ with ZnSe coverage. As additional ZnSe is deposited onto the *n*-type CuInSe$_2$ crystal surface, the CuInSe$_2$ valence band remains flat and the structure becomes dominated by the uppermost ZnSe bands. Hence, the VBO given by the different positions of ΔE_{vbm} in the clean and covered surface is $1.4 - 0.8 = 0.6$ eV.

The band offset can also be measured using Eq. (1). Figures 3(a) and 3(b) show the representative In 4*d* and Zn 3*d* cation core-level emission, respectively, for *n*-type CuInSe$_2$ as a function of the effective ZnSe coverage. The peak positions for clean CuInSe$_2$ is $E_{vbm-\text{In }4d}^{\text{CuInSe}_2} = 18.55 - E_F = 17.75$ eV while for the ZnSe surface $E_{vbm-\text{Zn }3d}^{\text{ZnSe}} = 10.65 - E_F = 9.25$ eV. The quantity $E_{\text{In }4d} - E_{\text{Zn }3d}$ across the heterojunction is measured for three coverages (7, 15, and 31 Å); the average over these is 7.72 ± 0.15 eV. From Eq. (1) we have $\Delta E_{vbm} = 17.75 - 9.25 - 7.72 = 0.78 \pm 0.15$ eV, within the range given by the alternative measurement (Fig. 2) i.e., 0.6 ± 0.1 eV. Bands may bend outside this interfacial region on a length scale of ≈ 1000 Å.

We have presented a theoretical prediction of the heterojunction band discontinuities of ZnSe/CuInSe$_2$ and the corroborating results of a synchrotron radiation soft x-ray photoemission investigation. The theoretical model predicts an offset of 0.60–0.70 eV depending on the strain conditions and establishes *p-d* coupling as the source of failure of the common-anion rule in ZnSe/CuInSe$_2$. The experimentally determined valence band discontinuity for this heterojunction is 0.7 ± 0.15 eV. Based on these results, a heterojunction band diagram for ZnSe on single-crystal *n*-type CuInSe$_2$ can be constructed.

[1] A. Rockett and R. W. Birkmire, J. Appl. Phys. **70**, R81 (1991).

[2] J. E. Jaffe and A. Zunger, Phys. Rev. B **28**, 5822 (1983).

[3] A. J. Nelson, A. Rockett, E. Colavita, M. Engelhardt, and H. Hochst, Phys. Rev. B **42**, 7518 (1990); R. S. Crisp, D. Haneman, and J. W. Chu, Solid State Commun. **78**, 465 (1991).

[4] K. Mitchell, C. Eberspacher, J. Ermer, and D. Pier, *Proceedings of the 20th IEEE Photovoltaic Specialists Conference*, Las Vegas (IEEE, New York, 1988), p. 1384.

[5] J. O. McCaldin, T. C. McGill, and C. A. Mead, Phys. Rev. Lett. **36**, 56 (1976).

[6] S.-H. Wei and A. Zunger, Phys. Rev. Lett. **59**, 144 (1987).

[7] W. A. Harrison, J. Vac. Sci. Technol. **14**, 1016 (1977); W. A. Harrison and J. Tersoff, J. Vac. Sci. Technol. B **4**, 1068 (1986).

[8] W. E. Spicer, P. W. Chye, P. R. Skeath, C. Y. Su, and I. Lindau, J. Vac. Sci. Technol. **16**, 1422 (1979).

[9] J. Tersoff, Phys. Rev. B **30**, 4874 (1984).

[10] M. Cardona and N. E. Christensen, Phys. Rev. B **35**, 6182 (1987).

[11] P. Hohenberg and W. Kohn, Phys. Rev. **136**, B864 (1964); W. Kohn and L. J. Sham, *ibid.* **140**, A1133 (1965).

[12] S.-H. Wei and H. Krakauer, Phys. Rev. Lett. **55**, 1200 (1985); and references therein.

[13] D. M. Ceperly and B. J. Alder, Phys. Rev. Lett. **45**, 566 (1980); J. P. Perdew and A. Zunger, Phys. Rev. B **23**, 5048 (1981).

[14] S. Froyen, Phys. Rev. B **39**, 3168 (1989).

[15] L. Garbato, F. Ledda, and R. Rucci, Prog. Cryst. Growth Charact. **15**, 1 (1987).

[16] *Landolt-Bornstein: Numerical Data and Functional Relationships in Science and Technology*, edited by O. Madelung, M. Schulz, and H. Weiss (Springer, Berlin, 1982), Vol. 17b.

[17] C. R. Schwerdtfeger and T. F. Ciszek, AIP Conf. Proc. **268**, 200 (1992).